Structure-Property Relationships in Commercial Polyetheretherketone Resins

Manuel Garcia-Leiner,[1] Maureen T.F. Reitman,[1] M. Jamal El-Hibri,[2] Ryan K. Roeder[3]
[1]*Exponent, Bowie, Maryland 20715*
[2]*Solvay Specialty Polymers, Alpharetta, Georgia 30005*
[3]*Department of Aerospace and Mechanical Engineering, Bioengineering Graduate Program, University of Notre Dame, Notre Dame, Indiana 46556*

Key relationships between molecular structure and final properties are reported for standard flow and high flow grades of commercially-available polyetheretherketone (PEEK) resins that differ primarily in molecular weight and molecular weight distribution. Despite similar chemistry and composition, the molecular size-dependent structural differences associated with the PEEK resins in this study are shown to influence the crystallization rate, final crystallinity, and melt rheology during processing, which subsequently affects mechanical properties, including strength, ductility, and impact resistance. These structure-property relationships provide fundamental understanding to aid in the design and manufacturing of industrial and medical devices that leverage both the advantages common to all PEEK resins, including chemical and thermal resistance, mechanical strength, and biocompatibility, as well as more subtle differences in crystallization kinetics, melt rheology, ductility, and impact resistance. **POLYM. ENG. SCI., 57:955–964, 2017.**

INTRODUCTION

Polyetheretherketone (PEEK) is a semi-crystalline thermoplastic with a linear, highly aromatic molecular structure including ether and ketone linkages [1–3]. PEEK exhibits unparalleled properties as compared to most other plastic resins. For example, PEEK exhibits excellent mechanical properties over a wide range of environmental conditions, including a high elastic modulus and ultimate strength coupled with post-yield ductility, and excellent creep resistance [1–6]. Moreover, PEEK exhibits excellent solvent resistance, thermal oxidative stability, and radiation resistance [1–6]. Because of these properties, PEEK can be sterilized by steam, ethylene oxide, and gamma radiation, and implantable grades are biocompatible and bioinert [5, 6]. PEEK is also readily fabricated into complex shapes and forms using traditional thermoplastic molding operations and readily compounded with fiber reinforcements (e.g., carbon, glass, etc.) or particulate fillers (e.g., barium sulfate, hydroxyapatite, etc.) for enhancing mechanical properties, radiopacity, and bioactivity [2–6]. Compared to metals, PEEK exhibits lower density, lower thermal, and electrical conductivity, greater corrosion resistance, and compatibility with X-rays and magnetic fields often used for quality control and diagnostic imaging [3–6]. Thus, for all the above reasons, PEEK has been used to replace metals, or in place of metals, in a growing number of industrial applications across the aerospace, automotive, biomedical, defense, electrical, electronics, energy, food processing, petroleum, and semiconductor industries [1–6].

Structure-property relationships for PEEK resins have been characterized using a wide variety of spectroscopic, thermal, mechanical, rheological, and microscopic techniques [2, 6–26]. These studies have reported relatively consistent behavior for neat PEEK resins and predictable effects of functional additives, which has contributed to the adoption of PEEK in applications requiring superior performance as compared to common polymeric resins. However, most previous studies have focused on the earliest commercial grades of PEEK resin (ICI or Victrex 450G and 150G) [2, 6–26]. PEEK, like most commercial polymers, is available from several suppliers and in several grades. Current commercially-available resins are polymerized using nucleophilic synthetic routes that include hydroquinone and 4,4′-difluorobenzophenone as starting monomers. In this reaction, the two difunctional monomers combine to create a linear polymer with a glass transition temperature (T_g) and melting temperature (T_m) around 145°C and 335°C, respectively [27–29]. Suppliers typically develop resin grades for specific markets, processes, or applications [3, 4]. Grade designation often encompasses neat resins, filled resins, and resins with different flow properties. While different flow properties can suggest different physical properties, only a few of these are described in the processing recommendations of comparable grades offered by various suppliers. A detailed understanding of these physical properties is required for the design and manufacturing of industrial and medical devices made with PEEK [29, 30].

Therefore, the objective of this study was to examine key structure-property relationships in current commercial, extrusion and injection molding grade, PEEK resins to improve understanding for the effects of the inherent polymer molecular structure and selected processing conditions on material properties. The molecular structure of the PEEK resins was characterized, including the composition, crystal structure, crystallinity, and molecular weight. Thermal, rheological, and mechanical properties were measured by standardized tests and analyzed in light of resin structural characteristics and processing history. We anticipate that improved understanding of the structure-property relationships associated with commercially-available PEEK resins will enable expanded use of PEEK in high performance applications by aiding design and manufacturing engineers.

EXPERIMENTAL

Materials

Standard (STD) and high flow (HF) grade PEEK resins were obtained from two resin suppliers: KetaSpire® KT-820 NT

Additional Supporting Information may be found in the online version of this article.

Correspondence to: M. Garcia-Leiner; e-mail: mgarcia-leiner@exponent.com
DOI 10.1002/pen.24472
Published online in Wiley Online Library (wileyonlinelibrary.com).

(STD-A) (Solvay Specialty Polymers USA, LLC), Victrex® 450G (STD-B) (Victrex PLC, UK), KetaSpire® KT-880 NT (HF-A), and Victrex® 150G (HF-B). STD-A and STD-B are standard extrusion flow grades, while HF-A and HF-B are high flow grades often recommended for injection molding applications, especially thin-walled moldings. For each test described below, materials were evaluated in the form of as-received resin pellets or as-molded shapes following supplier recommendations (Electronic Supporting Information, Table S1).

Chemical Composition

Chemical composition was characterized for as-molded flexural bars by Fourier transform infra-red (FTIR) spectroscopy with a standard (nonpolarized) IR beam using a Perkin Elmer Spectrum System 2000 FTIR spectrometer equipped with a diamond attenuated total reflectance (ATR) cell and a deuterated triglycine sulfate (DTGS) detector. Ten sequential scans were averaged for measurements on one lot sampled for each PEEK resin and grade.

Molecular Weight and Molecular Weight Distribution

The molecular weight (or molar mass) distribution was measured by gel permeation chromatography (GPC) in g/mol. As-received resin pellets were dissolved in a 1:1 mixture of phenol and 1,2,4-trichlorobenzene at elevated temperature. Samples were passed through Shodex HT-806M columns using a Polymer Laboratories PL-200 unit equipped with a differential refractive index detector and calibrated with narrow molecular weight polystyrene standards (Polymer Standards Services). The number average molecular weight (M_n), weight average molecular weight (M_w), *Z*-average molecular weight (M_z), $Z+1$ average molecular weight (M_{z+1}), and polydispersity indices (M_w/M_n, M_z/M_w) were reported to characterize the molecular weight distribution. Three lots were sampled for each PEEK resin and grade.

Crystal Structure and Crystallinity

Crystal structure and crystallinity were characterized for as-molded flexural bars by wide-angle X-ray diffraction (WAXD) using a horizontal Rigaku Geigerflex RU-200B diffractometer with nickel-filtered Cu Kα radiation (λ 1.542 Å) generated at 40 kV and 40 mA. Diffraction patterns were collected over 5° to 70° two-theta with a step size of 0.02° and step time of 1 s. Percent crystallinity was estimated from the 110, 111, 200, and 211 reflections, and the crystallite size was estimated from the most intense reflection (110), using established methods described in detail elsewhere [7, 14, 19]. Three lots were sampled for each PEEK resin and grade.

Thermal Properties and Crystallization

The thermal behavior of PEEK resins was characterized by differential scanning calorimetry (DSC) using a TA Instruments Q20 DSC. As-received resin pellets were subjected to two heating and cooling cycles at 20°C/min under nitrogen atmosphere. The enthalpy of fusion (ΔH_f) and characteristic thermal transitions, including the glass transition temperature (T_g), melting temperature (T_m), and crystallization temperature (T_c), were measured following ASTM D3418 [31]. Percent crystallinity was calculated from the measured enthalpy of fusion and the theoretical enthalpy of fusion for 100% crystalline PEEK, which was taken as 130 J/g [4, 6, 8]. Five and three lots were sampled for each STD and HF grade, respectively, for each PEEK resin. Dynamic crystallization was characterized under controlled thermal heating and cooling cycles by measuring the peak crystallization temperatures and corresponding crystallization times. In these experiments, samples were heated at 20°C/min until reaching 400°C and then cooled at rates ranging from 2 to 50°C/min. The crystallization temperature and time were measured at the peak of the crystallization exotherm and the temperature drop during crystallization, respectively. The crystallization time for a specific cooling rate was calculated as the time associated with twice the width of the crystallization exotherm at a position corresponding to one-half of its height. One lot was sampled for each PEEK resin and grade.

Rheological and Viscoelastic Properties

Resin rheology at high shear rates was measured for as-received resin pellets at 400°C following ASTM D3835 [32] using a Dynisco LCR-7000 capillary rheometer with a die 3.17 mm in height and 0.50 mm in diameter. Viscosity was measured over shear rates ranging 10^2 to 10^4 s^{-1}. Two lots were sampled for each PEEK resin and grade. Resin rheology at low shear rates and viscoelastic properties were measured by dynamic mechanical analysis (DMA) following ASTM D4440 [33] using a TA Instruments ARES RDA3 rheometer. The complex viscosity (η^*), loss modulus (G'), storage modulus (G''), and dissipation factor (tan δ) were measured over frequencies ranging 0.1–500 rad/s or temperatures ranging ~25°C–300°C. Frequency sweeps were measured for as-received resin pellets at 400°C using a 25 mm diameter parallel plate with a 1.5 mm gap. Two lots were sampled for STD grade PEEK resin. Temperature sweeps were measured for rectangular specimens, 50 mm in length and 1.27 mm in width, sectioned from the center of as-molded flexural bars, 3.2 mm in thickness, after annealing at 200°C for 2 h. Specimens were subjected to a cyclic 0.05% torsional strain at 1.6 Hz while heating at 5°C/min. Two and three lots were sampled for STD and HF grade PEEK resins, respectively.

Mechanical Properties

Tensile properties were measured for as-molded Type I tensile specimens, 3.2 mm in thickness, at a displacement rate of 5 and 50 mm/min using an Instron 5569 load frame and extensometer, following ASTM D638 [34]. The elastic modulus (*E*), yield strength (σ_y), yield elongation (ε_y), and elongation at break (ε_f) were measured from stress–strain curves. Three specimens per lot from three separate lots were tested for each PEEK resin and grade. Notched Izod impact resistance was measured for specimens prepared from as molded plaques, 3.2 mm in thickness, using a Testing Machines impact testing system, following ASTM D256 [35]. Notch sensitivity was investigated for specimens prepared with notch radii ranging from 0.08 to 0.76 mm. Five specimens per lot were tested for each notch radius, PEEK resin, and grade. Two and three lots were sampled for STD and HF grade PEEK resins, respectively. Instrumented impact testing was also performed with as molded disks, 3.2 mm in thickness and 102 mm in diameter, using a Dynatup 3000 drop-tower to measure the total energy absorption during high speed puncture,

 DOI 10.1002/pen

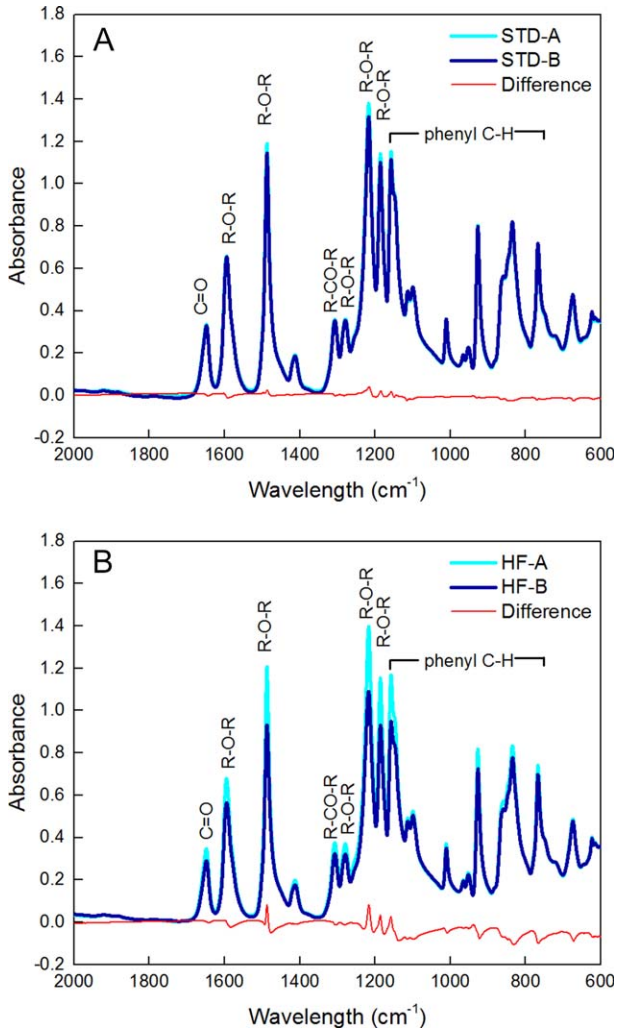

FIG. 1. Representative FTIR spectra showing characteristic absorptions for as-molded specimens prepared from (a) standard (STD) and (b) high flow (HF) grade commercial PEEK resins (A and B). [Color figure can be viewed at wileyonlinelibrary.com]

following ASTM D3763 [36]. Five specimens per lot from two separate lots were tested for each PEEK resin and grade.

Statistical Analysis

Properties measured on multiple samples and/or lots were reported as the pooled mean (±standard deviation). Two-way analysis of variance (ANOVA) (JMP 12, SAS Institute) was used to investigate the effects of the PEEK resin and grade on measured properties. *Post hoc* comparisons were performed using a Mann–Whitney *U*-test. Multiple analysis of covariance (MANCOVA) was used to investigate the effects of the PEEK resin, grade, and specimen notch size on notched Izod impact resistance after performing a log transform on the measured impact resistance to ensure a normal distribution. The level of significance for all tests was set at $p < 0.05$.

RESULTS AND DISCUSSION

Chemical Composition

FTIR spectra for each PEEK resin and grade exhibited characteristic absorptions corresponding to carbonyl groups of the ketone (~1,650 and 1,305 cm^{-1}), diphenyl ether linkages (~1,600, 1,490, 1,280, 1,215, 1,190 cm^{-1}), and aromatic hydrogens (~1,160 cm^{-1} and lower wavelength peaks) (Fig. 1). Differences between resins of the same grade were minor (Fig. 1), which suggests that the resins exhibited negligible differences in chemical composition. Moreover, characteristic absorptions were similar to those observed previously for the earliest commercial PEEK resins [16].

Molecular Weight and Molecular Weight Distribution

STD and HF grades of resin A exhibited a higher average molecular weight and lower polydispersity (narrower distribution) compared with resin B (Fig. 2 and Table 1). HF grades exhibited a lower average molecular weight as compared with STD grades ($p < 0.0001$, ANOVA), as expected (Fig. 2 and Table 1). However, the shape of the molecular weight distribution was similar for both STD and HF grades from the same resin supplier.

The molecular weight distribution of a PEEK resin affects the crystallinity [26, 29], crystallization kinetics [37–41], rheology [29, 37, 41], and mechanical properties [41–43], but few studies have reported the molecular weight distribution of

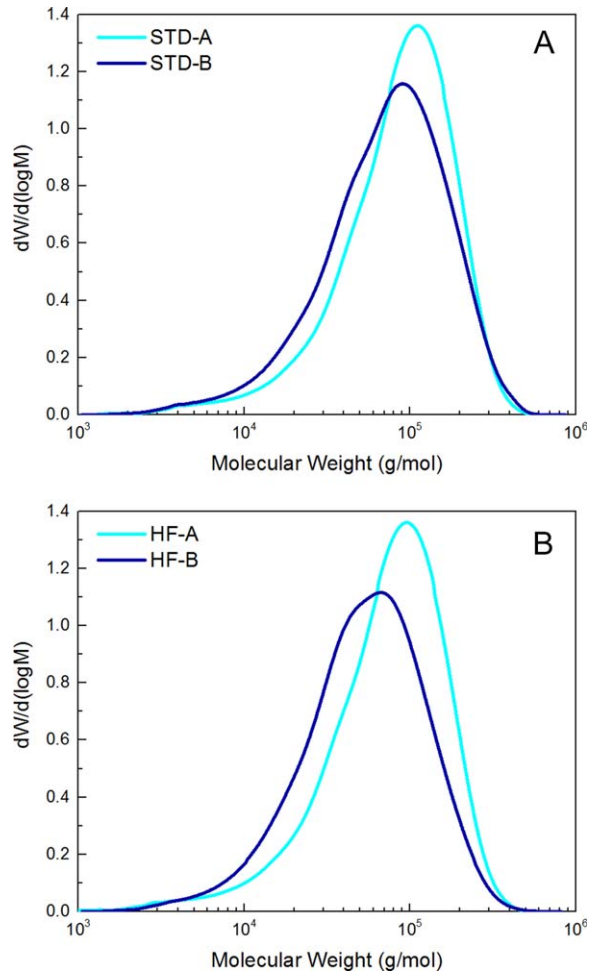

FIG. 2. Representative molecular weight distributions for (a) standard (STD) and (b) high flow (HF) grade commercial PEEK resins (A and B) measured by GPC on as-received resin pellets. Statistical parameters are reported in Table 1. [Color figure can be viewed at wileyonlinelibrary.com]

TABLE 1. Molecular weight distribution characterized by GPC for as-received resin pellets of standard (STD) and high flow (HF) grade commercial PEEK resins (A and B).

Grade-resin	M_n (g/mol)	M_w (g/mol)	M_w/M_n	M_z (g/mol)	M_z/M_w	M_{z+1} (g/mol)
STD-A	51,900 (300)*	107,300 (600)*	2.07 (0.01)*	153,600 (300)	1.43 (0.01)*	196,300 (100)*
STD-B	44,400 (700)*	98,300 (1800)*	2.22 (0.01)*	157,300 (3400)	1.60 (0.00)*	217,000 (5600)*
HF-A	40,000 (400)*	80,000 (1700)*	2.00 (0.03)*	120,500 (3400)	1.51 (0.02)*	163,400 (7500)*
HF-B	34,200 (500)*	72,500 (1100)*	2.12 (0.01)*	120,500 (1900)	1.66 (0.01)*	174,900 (2900)*

The mean (±standard deviation) is reported for three lots sampled for each PEEK resin and grade. Representative molecular weight distributions are shown in Fig. 2.

M_n = average molecular weight, M_w = weight average molecular weight, M_z = Z-average molecular weight, $M_{z+1} = Z + 1$ average molecular weight, M_w/M_n and M_z/M_w = polydispersity indices.

*$p < 0.05$ A versus B for same grade, Mann–Whitney U-test.

commercial PEEK resins. Characterization of the molecular weight distribution in aromatic polyketones is challenging due to an inherently strong chemical resistance, which limits solubility and direct assessment through traditional techniques such as GPC. In this study, PEEK resins were dissolved in an aromatic solvent mixture (phenol and 1,2,4-trichlorobenzene), which was previously demonstrated to enable accurate measurement of the average molecular weight of noncommercial PEEK resins by GPC as compared with light scattering using concentrated sulfuric acid as the solvent [11]. The measured differences in the average molecular weight and molecular weight distribution between commercial PEEK resins and grades are shown below to directly influence crystallinity, crystallization kinetics, rheology, and mechanical properties.

Crystal Structure and Crystallinity

WAXD patterns for each PEEK resin and grade exhibited characteristic reflections (110, 111, 200, 211) corresponding to an orthorhombic unit cell (Electronic Supporting Information, Fig. S1). The orthorhombic unit cell of PEEK contains only two-thirds of a repeat unit with measured dimensions reported as $a = 0.775$–0.788 nm, $b = 0.586$–0.594 nm, and $c = 0.988$–1.007 nm [7, 10, 14, 19]. The unit cell parameters of PEEK are not influenced by orientation and crystallization [23], unlike other polymorphic aromatic polyaryletherketones [44].

Differences in the crystallite size and percent crystallinity measured by WAXD for resins of the same grade were not statistically significant, except that STD-A exhibited ~3% lower percent crystallinity as compared with STD-B (Table 2). HF grades exhibited a larger crystallite size and greater percent crystallinity compared with STD grades ($p < 0.0005$, ANOVA), as expected (Table 2). HF grades exhibited a crystallite size in the (110) plane of ~16 nm and ~37% crystallinity as compared with ~15 nm and ~29%, respectively, for STD grades.

TABLE 2. Crystallite size and percent crystallinity measured by WAXD for as-molded specimens prepared from standard (STD) and high flow (HF) grade commercial PEEK resins (A and B).

Grade-resin	Crystallite size (nm)	Crystallinity (%)
STD-A	15.0 (0.0)	27.3 (0.8)*
STD-B	14.6 (0.6)	30.5 (0.4)*
HF-A	16.3 (0.6)	36.8 (1.2)
HF-B	16.3 (0.6)	37.3 (1.7)

The mean (±standard deviation) is reported for three lots sampled for each PEEK resin and grade. Representative WAXD spectra are shown in Fig. S2 (Supporting Information).

*$p < 0.05$ A versus B for same grade, Mann-Whitney U-test.

The crystal structure and crystallinity of PEEK are governed by molecular structure and processing, and in turn affect final properties (e.g., mechanical properties, dimensional stability, and chemical resistance), which ultimately dictate the suitability of a particular resin for a given application. Therefore, significant effort has been devoted to characterizing the crystal structure, crystallinity, and crystallization kinetics of PEEK. Crystallinity has been measured in the range of 0%–50%, depending on processing conditions, using various methods including WAXD [2, 6, 8–10, 17, 22, 23], DSC [2, 6, 13, 15–18, 22, 24, 29], FTIR [6, 9, 16, 17, 24], Raman spectroscopy [20], small angle X-ray scattering [8, 23], and nuclear magnetic resonance [25]. In this study, the decreased crystallinity of STD-A as compared with STD-B (~3% difference), as well as STD grades compared with HF grades (~8% difference), is most likely due to decreased chain mobility [26, 29, 37–41] in higher molecular weight resins and grades (Fig. 2 and Table 1) as processing conditions (thermal history) were similar between resins and grades (Tables S1, Supporting Information). The decreased crystallite size of STD as compared with HF grades was also most likely due decreased chain mobility in higher molecular weight resins, but may have also been influenced by other factors, such as paracrystallinity [45].

Thermal Properties and Crystallization

Thermal transitions measured by DSC under cooling and heating cycles (Electronic Supporting Information, Fig. S2) were used to determine the crystallization temperature, glass transition temperature, melting temperature, and percent crystallinity (Table 3). STD and HF grades of resin A exhibited a lower crystallization temperature as compared with resin B by ~6°C and ~8°C, respectively (Table 3). STD and HF grades of resin A also exhibited lower crystallinity as compared with resin B by ~3% and ~5%, respectively (Table 3). Under dynamic crystallization, STD and HF grades of resin A exhibited decreased crystallization kinetics as compared with resin B, and the magnitude of the difference increased with increased crystallization temperature (Fig. 3). HF grades exhibited a higher crystallization temperature and crystallinity (Table 3, $p < 0.0001$, ANOVA), as well as more rapid crystallization kinetics (Fig. 3), compared with STD grades, as expected.

DOI 10.1002/pen

TABLE 3. Thermal transitions and percent crystallinity measured by DSC for as-received resin pellets of standard (STD) and high flow (HF) grade commercial PEEK resins (A and B).

Grade-resin	T_g (°C)	T_c (°C)	T_m (°C)	ΔH_f (J/g)	Crystallinity (%)
STD-A	152.3 (1.2)	282.4 (1.0)*	338.9 (0.7)*	48.3 (1.1)*	37.1 (0.8)*
STD-B	151.2 (1.2)	287.8 (1.2)*	340.3 (0.6)*	52.1 (2.8)*	40.0 (2.1)*
HF-A	148.8 (0.2)*	287.9 (4.4)*	340.1 (0.6)*	58.6 (2.3)*	45.1 (1.8)*
HF-B	146.9 (0.7)*	295.8 (0.9)*	342.1 (0.4)*	65.2 (2.1)*	50.2 (1.6)*

The mean (±standard deviation) is reported for five and three lots sampled for each STD and HF grade, respectively, for each PEEK resin. Representative DSC curves are shown in Fig. S3 (Supporting Information).

T_g = glass transition temperature, T_c = crystallization temperature, T_m = melting temperature, ΔH_f = enthalpy of fusion.

*$p < 0.05$ A versus B for same grade, Mann–Whitney U-test.

The crystallization temperature, crystallinity, and crystallization kinetics were decreased for resin A compared with resin B, and for STD compared with HF grades (Table 3, Fig. S2 [Supporting Information], and Fig. 3). Note that the ASTM standard test method includes an initial heating cycle to erase prior thermal history [31]. Therefore, differences in the crystallinity measured by DSC (Table 3) as compared with WAXD (Table 2) reflect differences in prior thermal history. Moreover, differences in crystallinity between resins and grades were more prominent when measured by DSC and reflect the effect of molecular structure rather than thermal history. Therefore, these results suggest that chain mobility was decreased in higher molecular weight resins and grades (Fig. 2 and Table 1), resulting in a decreased crystallization temperature, crystallinity, and crystallization kinetics (Table 3). Crystallization of PEEK is highly dependent on the mobility of molecular chains and their ability to organize during cooling of the melt, such that lower molecular weight resins and grades crystallize more readily [26, 29, 37–41]. Thus, lower molecular weight grades and resins were able to crystallize at higher temperatures (Table 3 and Fig. 3) independent of prior thermal history.

The measured thermal transitions of STD-B were similar to the earliest commercial grades of the same PEEK resin, which were reported to exhibit a glass transition temperature above 145°C, a melt crystallization temperature of ~290°C, and a melting temperature of ~340°C [2]. The ASTM standard for implantable grades of PEEK specifies a glass transition temperature of 125°C–165°C, a melt crystallization temperature of 260–320°C, and a melting temperature of 320°C–360°C, each measured by DSC at a specified heating/cooling rate of 20°C/min [46]. Using the same methods, the commercial resins and grades in this study exhibited a glass transition temperature of ~145°C–155°C, a melt crystallization temperature of ~280°C–300°C, and a melting temperature of ~335°C–345°C. The greater ranges in the ASTM specification are due to the recognition that the thermal properties and crystallization of PEEK is strongly influenced by molecular structure, which may be tailored for the development of new resins/grades for new or existing applications.

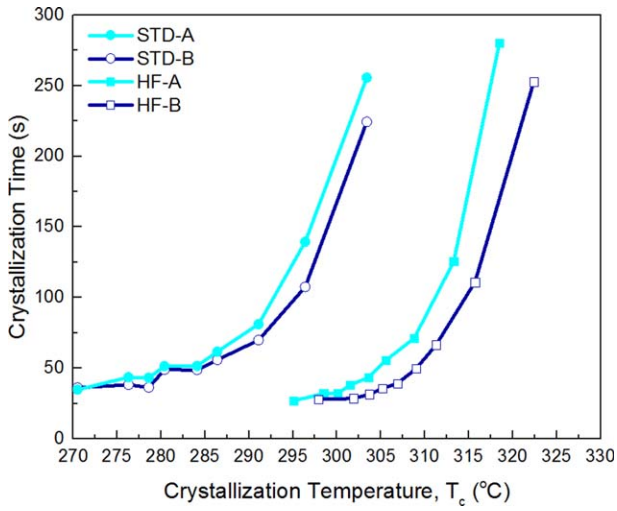

FIG. 3. Dynamic crystallization of standard (STD) and high flow (HF) grade commercial PEEK resins (A and B) showing the crystallization kinetics measured by DSC on as-received resin pellets. [Color figure can be viewed at wileyonlinelibrary.com]

Thermal transitions and the crystallization behavior of PEEK resins measured by DSC have been extensively reported, and are known to be highly dependent on both molecular mobility and the heating/cooling rate [2, 6–8, 13, 15–18, 22–24, 26, 29–31, 37–41, 47]. For example, cold crystallization is observed at temperatures close to 180°C under slow heating rates [2]. PEEK crystallization during cooling occurs in multiple stages and is highly dependent on the cooling rate [2]. Thus, molecular structure and processing both govern the thermal properties and crystallization of PEEK, which in turn affects rheological and, via the spherulitic morphology, mechanical properties, respectively [2, 6, 29, 41]. Moreover, differences in thermal properties and crystallization behavior must be taken into account when optimizing melt processing conditions for a given PEEK resin and grade.

Rheology and Viscoelastic Properties

The melt viscosity measured by capillary rheometry at high shear rates, typical of melt processing methods such as extrusion and injection molding (>200 1/s), exhibited shear thinning with increased shear rate for each PEEK resin and grade (Fig. 4). The melt viscosity and overall behavior was similar for PEEK resins of the same grade. However, STD and HF grades of resin A exhibited slightly lower viscosity at moderate shear rates (~100–400 1/s), as well as less shear thinning with increased shear rate, as compared with resin B (Fig. 4). STD grades exhibited a higher melt viscosity as compared with HF grades (Fig. 4), as expected.

The complex viscosity measured by dynamic oscillatory rheometry for STD resins at low shear rates also exhibited shear thinning (Fig. 5a). STD-A exhibited lower viscosity at low

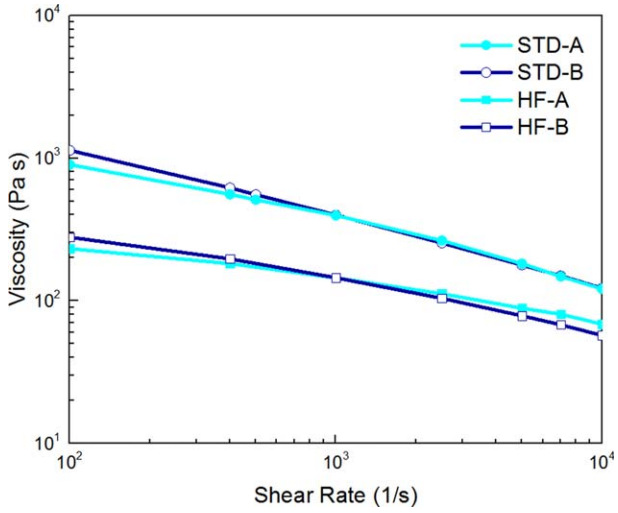

FIG. 4. High shear rheology of standard (STD) and high flow (HF) grade commercial PEEK resins (A and B) showing the effect of shear rate on melt viscosity measured by capillary rheometry on as-received resin pellets at 400°C. [Color figure can be viewed at wileyonlinelibrary.com]

frequencies, as well as less shear thinning with increased frequency, as compared with STD-B (Fig. 5a). The measured dynamic moduli were also lower for STD-A as compared with STD-B and the difference between resins was more pronounced at lower frequency (Fig. 5b). The difference between the storage (G') and loss (G'') modulus was greater for STD-A as compared with STD-B and more pronounced lower frequencies corresponding to the flow region (Fig. 5b).

Viscoelastic properties measured by DMA on solid specimens of STD resins (Fig. 6) also reflected behavior observed in the melt (Fig. 5b). STD and HF grades of resin A exhibited a slightly greater glass transition temperature compared with resin B by ~4°C and ~1°C, respectively (Fig. 6b and d). At temperatures below the glass transition, the storage modulus measured for STD and HF grades of resin A was less temperature sensitive as compared to resin B (Fig. 6a and c). HF grades exhibited smaller, almost negligible, differences between resins in the glass transition temperature, as well as the temperature sensitivity of the storage modulus at temperatures below the glass transition temperature, as compared with STD grades (Fig. 6).

Melt viscosity, shear thinning, and viscoelasticity were decreased for resin A as compared with resin B at low and moderate shear rates, while melt viscosity was increased for STD compared with HF grades at moderate and high shear rates (Figs. 4–6). These results suggest that measured differences in rheological properties were most likely due to differences in the molecular weight distribution between PEEK resins and grades. Increased molecular weight results in decreased chain mobility or increased chain entanglement [29]. Therefore, melt viscosity was decreased for resin A compared with resin B at low and moderate shear rates (Figs. 4 and 5a) due to the greater average molecular weight of resin A compared with resin B (Table 1). Melt viscosity was also decreased for STD compared with HF grades at moderate and high shear rates (Fig. 4) due to the greater average molecular weight of STD as compared with HF grades (Table 1). Greater polydispersity creates a disparity in rheological behavior between smaller chains and longer, highly-entangled chains, which affects macroscopic flow in the terminal region. Therefore, shear thinning and viscoelasticity were decreased for resin A as compared with resin B at low and moderate shear rates (Figs. 4–6) due to the lower polydispersity of resin A as compared with resin B (Table 1). The ratio of dynamic moduli is well-known to be sensitive to differences in polydispersity or branching [29]. Increased polydispersity in the molecular weight distribution was previously shown to increase shear thinning and viscoelastic damping behavior in PEEK resins [29].

PEEK resins can be converted to useful forms using conventional melt processing methods, such as extrusion and injection molding, despite exhibiting a high melting temperature. Therefore, the characterization of rheological properties above the melting temperature, typically at 375°C–400°C, is critical for process optimization and resin selection [29]. The results of this study demonstrate a prominent effect of the resin molecular weight distribution on rheological and viscoelastic properties.

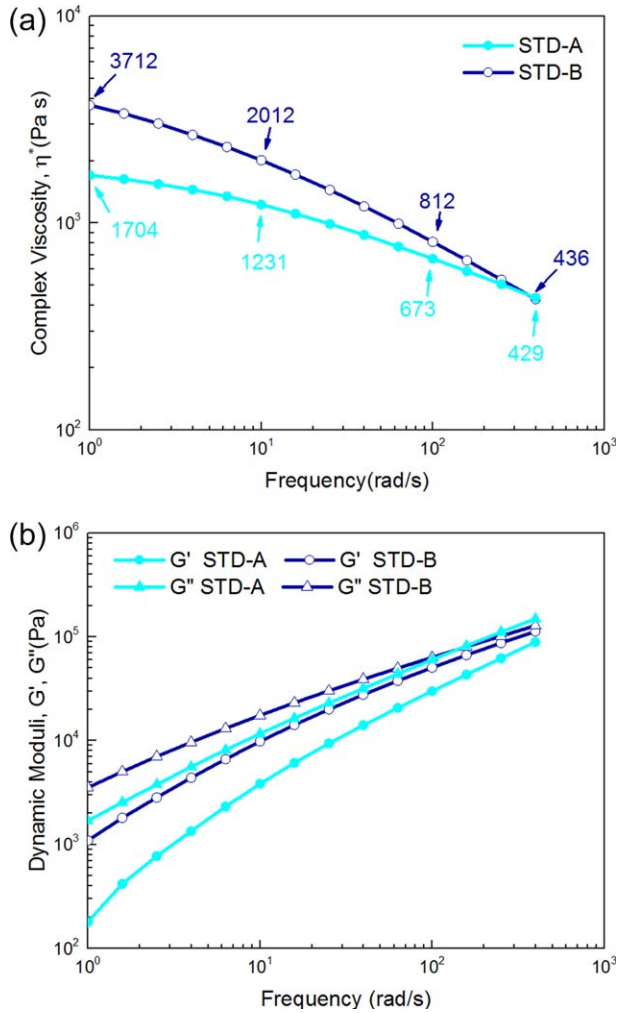

FIG. 5. Low shear rheology of standard (STD) grade commercial PEEK resins (A and B) showing the effect of loading frequency on the (a) complex viscosity (η^*) and (b) dynamic moduli, including the loss (G') and storage (G'') modulus, measured by dynamic, parallel plate rheometry on as-received resin pellets at 400°C. [Color figure can be viewed at wileyonlinelibrary.com]

DOI 10.1002/pen

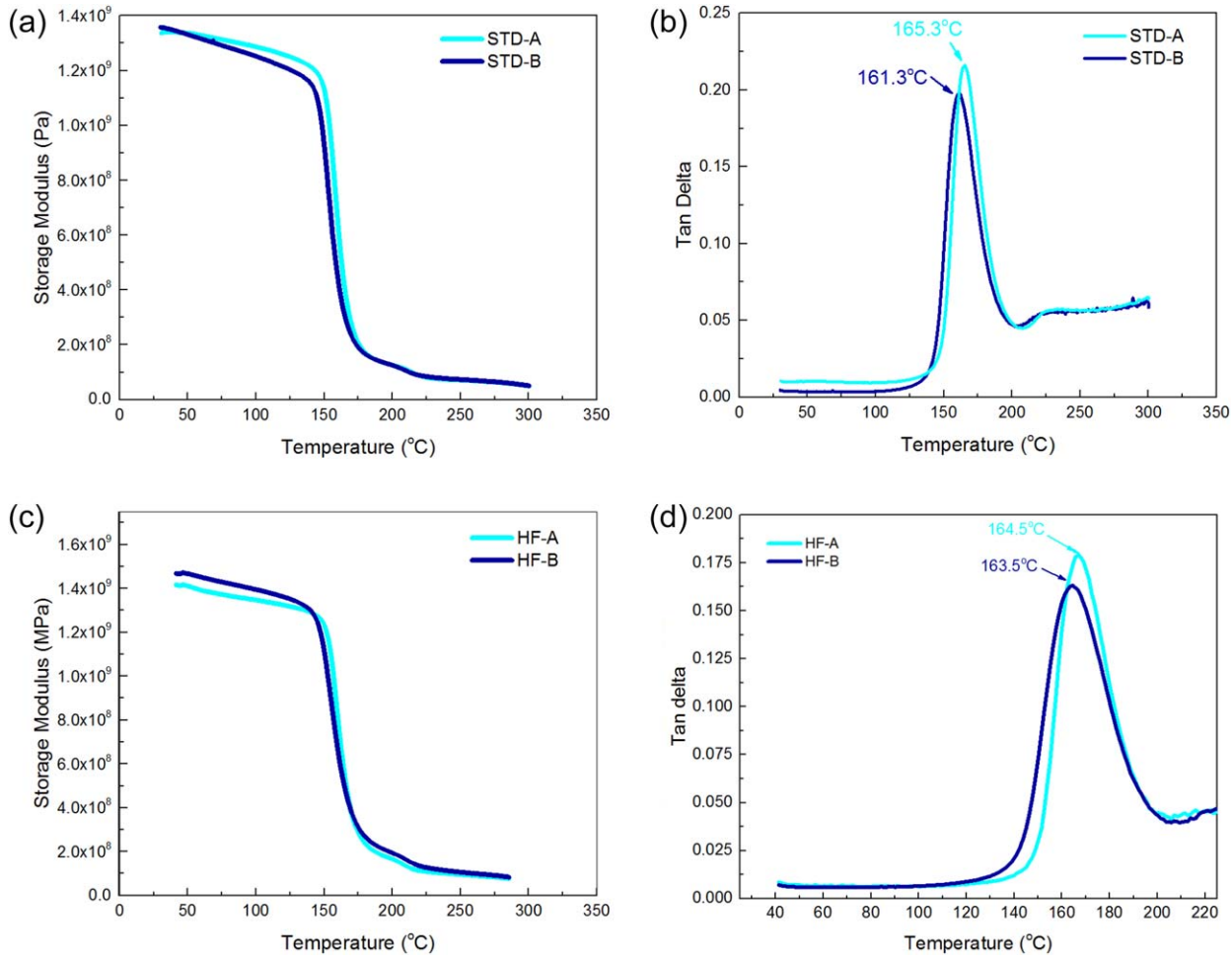

FIG. 6. Viscoelastic properties of standard (STD) and high flow (HF) grade commercial PEEK resins (A and B) measured by DMA on as-molded specimens showing the effect of temperature on the (a, c) storage modulus (G'') and (b, d) dissipation factor (tan δ). [Color figure can be viewed at wileyonlinelibrary.com]

Mechanical Properties

Stress–strain curves measured for as-molded specimens loaded in uniaxial tension exhibited behavior typical of ductile high performance resins, including yielding and cold drawing prior to fracture (Fig. 7). HF resins exhibited a larger drop in stress and more distinct transition to cold drawing behavior compared with STD resins (Fig. 7). Tensile properties were measured from stress–strain curves for each PEEK resin and grade (Table 4). STD-A exhibited a slightly lower yield strength and yield elongation (~1%–4% relative difference) as compared with STD-B (Table 4). In contrast, STD-A exhibited a greater elongation at break (>50% relative difference) compared with STD-B, but the difference at the higher displacement rate was not statistically significant (Table 4). HF-A exhibited a slightly lower elastic modulus (~5%–6% relative difference), but significantly greater elongation at break (>200% at 5 mm/min and >40% at 50 mm/min) as compared with HF-B (Table 4). All other differences in tensile properties between resins of the same grade were not statistically significant. STD grades exhibited a decreased elastic modulus and yield properties ($p < 0.05$, ANOVA) as compared with HF grades (Table 4). Yield properties and elongation at break were sensitive to the displacement rate ($p < 0.0001$, MANOVA) for both resins and grades (Table 4).

The impact resistance of each PEEK resin and grade was assessed by notched Izod specimens of varying notch radii (Fig. 8) and total energy absorption during high speed puncture (Table 5). Izod impact resistance increased with an increased notch radius ($p < 0.0001$, ANCOVA) for each PEEK resin and grade (Fig. 8), as expected. Resin A exhibited a greater Izod impact resistance ($p < 0.0001$, ANCOVA) and decreased notch sensitivity ($p < 0.0005$, ANCOVA) compared with resin B for STD grades, but differences between HF grades were not statistically significant (Fig. 8). STD grades exhibited a greater Izod impact resistance ($p < 0.0001$, ANCOVA) compared with HF grades (Fig. 8), as expected. Total energy absorption during puncture was also greater for STD and HF grades resin A compared with resin B, but differences were lower in HF grades compared with STD grades (Table 5). STD grades exhibited greater total energy absorption during puncture compared with HF grades for resin A ($p < 0.001$, Mann–Whitney U-test), but not resin B (Fig. 8).

STD and HF grades of resin A generally exhibited lower strength, greater ductility, and greater impact resistance

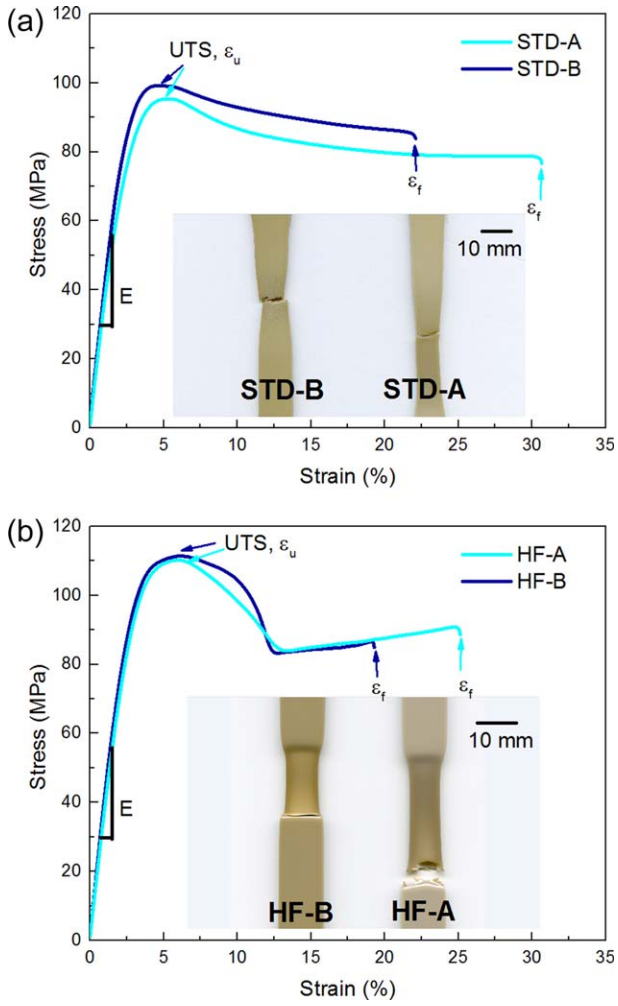

FIG. 7. Tensile properties of (a) standard (STD) and (b) high flow (HF) grade commercial PEEK resins (A and B) showing representative stress-strain curves for as-molded specimens loaded in uniaxial tension under ambient conditions and images of failed specimens. The elastic modulus (E), ultimate tensile strength (UTS), ultimate strain (ε_u), and strain to failure (ε_f) are labeled on stress–strain curves. Selected tensile property measurements are reported in Table 4. [Color figure can be viewed at wileyonlinelibrary.com]

compared with resin B, while STD grades generally exhibited lower strength, lower ductility, and greater impact resistance as compared with HF grades (Figs. 7 and 8 and Tables 4 and 5). The measured differences in these mechanical properties were most likely due to differences in crystallinity and the molecular weight distribution between PEEK resins and grades, as processing conditions (thermal history) were similar between resins and grades (Tables S1, Supporting Information). Strength was decreased for resin A as compared with resin B and for STD compared with HF grades (Table 4) due to the lower crystallinity of resin A compared with resin B and STD compared with HF grades, respectively (Tables 2 and 3). Recall, however, that these differences in crystallinity were due to the greater average molecular weight of resin A compared with resin B and STD compared with HF grades (Table 1). Therefore, differences in strength were primarily and directly governed by crystallinity, but indirectly governed by molecular weight. Ductility (Table 4) and impact resistance (Fig. 8 and Table 5) were increased for resin A compared with resin B due to the greater average molecular weight of resin A compared with resin B (Table 1) as differences in crystallinity were relatively small by comparison. Impact resistance was also increased for STD as compared with HF grades (Fig. 8 and Table 5) due to the greater average molecular weight of STD compared with HF grades (Table 1). The greater difference in impact resistance between resin A and B for the STD compared with the HF grade (Fig. 8 and Table 5) was most likely due to the greater difference in molecular weight and crystallinity between resin A and B for the STD grade compared with the HF grade (Tables 1–3). Therefore, these results suggest that chain entanglement was increased in higher molecular weight resins and grades (Table 1), resulting in increased impact resistance (Fig. 8 and Table 5).

The measured mechanical properties of resin B were similar to previous data for commercial grades of the same resin, which were reported to exhibit a tensile modulus of ~4 GPa, a tensile yield strength of ~90–100 MPa, an elongation at break of ~25%–45%, and an Izod impact resistance of 50–75 J/m for a 0.25 mm notch radius [2, 4, 5, 41, 43]. The ASTM standard for implantable grades of PEEK specifies a tensile yield strength >90 MPa, an elongation at break >5%, and an Izod impact resistance >50 J/m for a 0.25 mm notch radius [46]. Using the same methods, the commercial resins and grades in this study

TABLE 4. Tensile properties measured for as-molded specimens prepared from standard (STD) and high flow (HF) grade commercial PEEK resins (A and B).

Grade-resin	Displacement rate (mm/min)	Elastic modulus (GPa)	Yield strength (MPa)	Yield elongation (%)	Elongation at break (%)
STD-A	5	3.79 (0.07)	89.5 (0.7)*	4.91 (0.04)*	73 (7)*
STD-B	5	3.89 (0.23)	92.6 (1.1)*	5.03 (0.02)*	48 (9)*
HF-A	5	3.84 (0.03)*	98.6 (0.7)	5.57 (0.06)	120 (17)*
HF-B	5	4.06 (0.02)*	98.9 (0.8)	5.73 (0.12)	55 (15)*
STD-A	50	3.74 (0.12)	94.8 (0.4)*	5.17 (0.02)*	37 (16)
STD-B	50	3.95 (0.21)	98.2 (0.4)*	5.22 (0.02)*	21 (1)
HF-A	50	3.80 (0.01)*	103.5 (0.7)	5.73 (0.06)	27 (1)*
HF-B	50	4.04 (0.02)*	104.6 (0.4)	5.80 (0.10)	19 (1)*

The pooled mean (±standard deviation) is reported for three specimens per lot from three separate lots sampled for each PEEK resin and grade. Representative stress–strain curves are shown in Fig. 7.

*$p < 0.05$ A versus B for same grade and displacement rate, Mann–Whitney U-test.

DOI 10.1002/pen

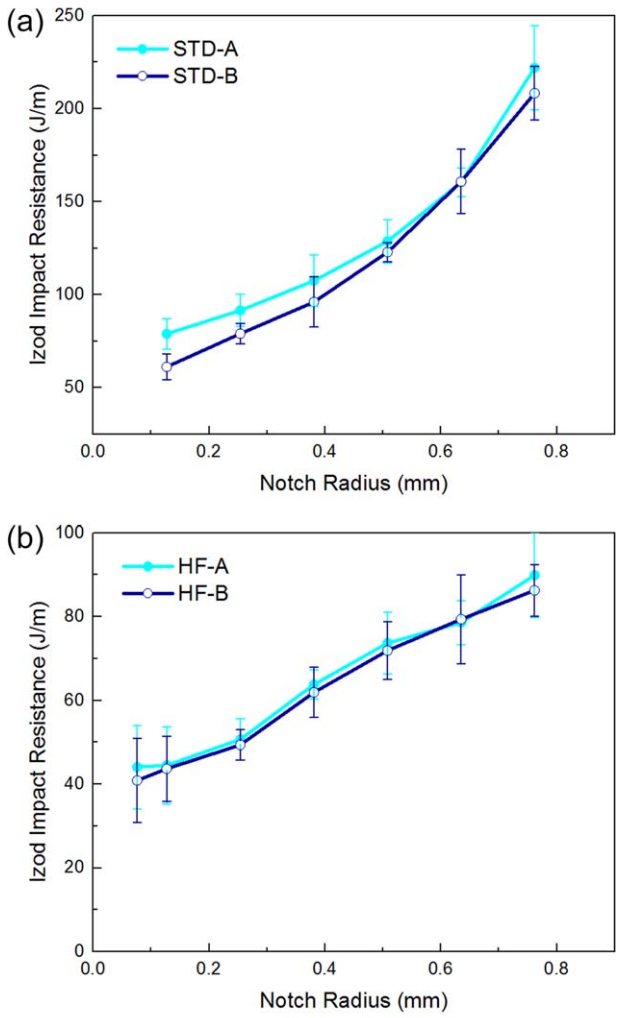

FIG. 8. Impact resistance of as-molded, notched Izod specimens prepared from (a) standard (STD) and (b) high flow (HF) grade commercial PEEK resins (A and B) showing the effect of the notch radius. [Color figure can be viewed at wileyonlinelibrary.com]

exhibited a tensile yield strength of ~90–105 MPa, an elongation at break of ~20%–120%, and an Izod impact resistance of ~50–90 J/m for a 0.25 mm notch radius. Therefore, each PEEK resin and grade examined in this study was able to meet the ASTM specification.

TABLE 5. Total energy absorption during high speed puncture measured for as-molded disks prepared from standard (STD) and high flow (HF) grade commercial PEEK resins (A and B).

Grade	Total energy absorption (J)
STD-A	84.9 (4.3)*
STD-B	74.7 (1.8)*
HF-A	77.8 (1.8)*
HF-B	75.6 (2.7)*

The pooled mean (±standard deviation) is reported for five specimens per lot from two separate lots sampled for each PEEK resin and grade.
*$p < 0.05$ A versus B for same grade, Mann–Whitney U-test.

PEEK resins exhibit superior mechanical properties compared to most commercially available thermoplastic materials [1–6]. However, the mechanical properties of PEEK resins are known to be highly dependent on intrinsic factors, such as the molecular weight [4, 41–43], crystallinity [37, 43], and processing methods (thermal history) [13, 17, 42, 43], and extrinsic factors, such as the strain rate [5, 6], temperature [2, 5, 12, 21], and notch radius [6, 13, 48]. Therefore, each of these factors must be taken into careful consideration for resin selection. The results of this study highlight the effect of the resin molecular weight distribution on tensile properties and impact resistance, via crystallization and the spherulitic morphology [30, 42], which must be taken into account for resin selection and process optimization, especially in complex designs where enhanced ductility and impact resistance may be desirable to increase durability of the final part.

CONCLUSIONS

A comprehensive investigation of key structure-property in standard flow and high flow grades of commercial PEEK resins revealed differences that were primarily derived from the resin molecular weight distribution and associated molecular mobility or entanglement. The decreased chain mobility (or increased entanglement) associated with increased resin molecular weight resulted in decreased crystallization kinetics and final crystallinity; decreased melt viscosity, shear thinning, and viscoelasticity; and decreased strength, increased ductility, increased impact resistance, and decreased notch sensitivity. These structure-property relationships provide fundamental understanding to aid in the design and manufacturing of industrial and medical devices that leverage both the advantages common to all PEEK resins, including chemical and thermal resistance, mechanical strength, and biocompatibility, as well as more subtle differences in crystallization kinetics, melt rheology, ductility, and impact resistance.

ACKNOWLEDGMENTS

The authors acknowledge Edward M. Buckwald, Judy Melville, and Shawn Shorrock of Solvay Specialty Polymers for supporting all aspects of sampling, testing, and data compilation for this manuscript.

REFERENCES

1. F. Herold and A. Schneller, *Adv. Mater.*, **4**, 143 (1992).
2. H.X. Nguyen and H. Ishida, *Polym. Compos.*, **8**, 57 (1987).
3. J.K. Fink, *High Performance Polymers*, William Andrew, Norwich, NY (2008).
4. D. Kemmish, *Update on the Technology and Applications of Polyaryletherketones*, Smithers Rapra, Shawbury, UK (2010).
5. S.M. Kurtz and J. Devine, *Biomaterials*, **28**, 4845 (2007).
6. S.M. Kurtz, Ed., *PEEK Biomaterials Handbook*, Elsevier, Amsterdam (2012).
7. P.C. Dawson and D.J. Blundell, *Polymer*, **21**, 577 (1980).
8. D.J. Blundell and B.N. Osborn, *Polymer*, **24**, 953 (1983).
9. J.M. Chalmers, W.F. Gaskin, and M.W. Mackenzie, *Polym. Bull.*, **11**, 433 (1984).

10. J.N. Hay, D.J. Kemmish, J.I. Langford, and A.I.M. Rae, *Polym. Commun*., **25**, 175 (1984).
11. J. Devaux, D. Delimoy, R. Legras, J.P. Mercier, C. Strazielle, and E. Nield, *Polymer*, **26**, 1994 (1985).
12. D.P. Jones, D.C. Leach, and D.R. Moore, *Polymer*, **26**, 1385 (1985).
13. D.J. Kemmish and J.N. Hay, *Polymer*, **26**, 905 (1985).
14. S. Kumar, D.P. Anderson, and W.W. Adams, *Polymer*, **27**, 329 (1986).
15. Y.C. Lee and R.S. Porter, *Polym. Eng. Sci*., **26**, 633 (1986).
16. H.X. Nguyen and H. Ishida, *Polymer*, **27**, 1400 (1986).
17. P. Cebe, S.Y. Chung, and S.D. Hong, *J. Appl. Polym. Sci*., **33**, 487 (1987).
18. Y. Deslandes, M. Day, N.-F. Sabir, and T. Suprunchuk, *Polym. Compos*., **10**, 360 (1989).
19. D.J. Blundell and A.B. Newton, *Polymer*, **32**, 308 (1991).
20. N.J. Everall, J. Lumsdon, J.M. Charles, and N. Mason, *Spectrochim. Acta*, **47A**, 1305 (1991).
21. M. Brillhart and J. Botsis, *Polymer*, **33**, 5225 (1992).
22. A.A. Mehmet-Alkan and J.N. Hay, *Polymer*, **33**, 3527 (1992).
23. B.S. Hsiao, K.H. Gardner, D.Q. Wu, and B. Chu, *Polymer*, **34**, 3986 (1993).
24. H.J. Cha and C.W. Frank, *Korea Polym. J*., **7**, 141 (1999).
25. N.J. Clayden, *Polymer*, **41**, 1167 (2000).
26. Q. Lu, Z. Yang, X. Li, S. Jin, *J. Appl. Polym. Sci*, **114**, 2060 (2009).
27. R.N. Johnson, A.G. Farnham, R.A. Clendinning, W.F. Hale, and C.N. Merriam, *J. Polym. Sci. Part A-1: Polym. Chem*., **5**, 2375 (1967).
28. T.E. Attwood, P.C. Dawson, J.L. Freeman, L.R.J. Hoy, J.B. Rose, and P.A. Staniland, *Polymer*, **22**, 1096 (1981).
29. K.L. White, L. Jin, N. Ferrer, M. Wong, T. Bremner, and H.-J. Sue, *Polym. Eng. Sci*, **53**, 651 (2013).
30. F.J. Medellin-Rodriguez and P.J. Phillips, *Polym. Eng. Sci*., **30**, 860 (1990).
31. ASTM D3418-08, *Standard Test Method for Transition Temperatures and Enthalpies of Fusion and Crystallization of Polymers by Differential Scanning Calorimetry*, ASTM International, West Conshohocken, PA (2008).
32. ASTM D3835-08, *Standard Test Method for Determination of Properties of Polymeric Materials by Means of a Capillary Rheometer*, ASTM International, West Conshohocken, PA (2008).
33. ASTM D4440-01, *Standard Test Method for Plastics: Dynamic Mechanical Properties Melt Rheology*, ASTM International, West Conshohocken, PA (2001).
34. ASTM D638-03, *Standard Test Method for Tensile Properties of Plastics*, ASTM International, West Conshohocken, PA (2003).
35. ASTM D256-02, *Standard Test Methods for Determining the Izod Pendulum Impact Resistance of Plastics*, ASTM International, West Conshohocken, PA (2002).
36. ASTM D3763-06, *Standard Test Method for High Speed Puncture Properties of Plastics Using Load and Displacement Sensors*, ASTM International, West Conshohocken, PA (2006).
37. J.N. Hay and D.J. Kemmish, *Plast. Rubber Process. Appl*., **11**, 29 (1989).
38. A. Jonas and R. Legras, *Polymer*, **32**, 2691 (1991).
39. M. Day, Y. Deslandes, J. Roovers, and T. Suprunchuk, *Polymer*, **32**, 1258 (1991).
40. Y. Deslandes, F.N. Sabir, and J. Roovers, *Polymer*, **32**, 1267 (1991).
41. M. Yuan, J.A. Galloway, R.J. Hoffman, and S. Bhatt, *Polym. Eng. Sci*., **51**, 94 (2010).
42. J.N. Chu and J.M. Schultz, *J. Mater. Sci*., **25**, 3746 (1990).
43. R.A. Chivers and D.R. Moore, *Polymer*, **35**, 110 (1994).
44. M. Garcia-Leiner, B. Clay, and P. Ricou, *Society of Plastics Engineers Annual Technical Conference (ANTEC)*, Society of Plastics Engineers, Bethel, CT, 1587076 (2013).
45. P. Cebe, L. Lowry, S.Y. Chung, A. Yavrouian, and A. Gupta, *J. Appl. Polym. Sci*., **34**, 2273 (1987).
46. ASTM F2026-16, *Standard Specification for Polyetheretherketone (PEEK) Polymers for Surgical Implant Applications*, ASTM International, West Conshohocken, PA (2016).
47. C.N. Velisaris and J.C. Seferis, *Polym. Eng. Sci*., **26**, 1574 (1986).
48. M. Sobieraj, J.E. Murphy, J.G. Brinkman, S. Kurtz, and C. Rimnac, *Biomaterials*, **31**, 9156 (2010).

 DOI 10.1002/pen